UC Riverside
UC Riverside Previously Published Works

Title

Fundamentally different global marine nitrogen cycling in response to severe ocean deoxygenation

Permalink

Journal

ISSN

Authors

Naafs, B David A
Monteiro, Fanny M
Pearson, Ann
et al.

Publication Date

DOI

Peer reviewed

Fundamentally different global marine nitrogen cycling in response to severe ocean deoxygenation

B. David A. Naafs[a,1,2], Fanny M. Monteiro[b,1], Ann Pearson[c], Meytal B. Higgins[d], Richard D. Pancost[a], and Andy Ridgwell[b,e]

[a]Organic Geochemistry Unit, School of Chemistry, School of Earth Sciences, Cabot Institute for the Environment, University of Bristol, Bristol BS8 1TA, United Kingdom; [b]School of Geographical Sciences, University of Bristol, Bristol BS8 1SS, United Kingdom; [c]Department of Earth and Planetary Sciences, Harvard University, Cambridge, MA 02138; [d]ExxonMobil Research & Engineering, Annandale, NJ 08801; and [e]Department of Earth and Planetary Sciences, University of California, Riverside, CA 92521

The present-day marine nitrogen (N) cycle is strongly regulated by biology. Deficiencies in the availability of fixed and readily bioavailable nitrogen relative to phosphate (P) in the surface ocean are largely corrected by the activity of diazotrophs. This feedback system, termed the "nitrostat," is thought to have provided close regulation of fixed-N speciation and inventory relative to P since the Proterozoic. In contrast, during intervals of intense deoxygenation such as Cretaceous ocean anoxic event (OAE) 2, a few regional sedimentary $\delta^{15}N$ records hint at the existence of a different mode of marine N cycling in which ammonium plays a major role in regulating export production. However, the global-scale dynamics during this time remain unknown. Here, using an Earth System model and taking the example of OAE 2, we provide insights into the global marine nitrogen cycle under severe ocean deoxygenation. Specifically, we find that the ocean can exhibit fundamental transitions in the species of nitrogen dominating the fixed-N inventory—–from nitrate (NO_3^-) to ammonium (NH_4^+)—and that as this transition occurs, the inventory can partially collapse relative to P due to progressive spatial decoupling between the loci of NH_4^+ oxidation, NO_3^- reduction, and nitrogen fixation. This finding is relatively independent of the specific state of ocean circulation and is consistent with nitrogen isotope and redox proxy data. The substantive reduction in the ocean fixed-N inventory at an intermediate state of deoxygenation may represent a biogeochemical vulnerability with potential implications for past and future (warmer) oceans.

nitrogen | ocean | OAE | Cretaceous | anthropogenic

Nitrogen (N) is an essential nutrient for life, and in the modern ocean, small regional differences in the bioavailability of N induce large differences in primary productivity, ecosystem dynamics, and biogeochemical cycles (1–3). The ocean inventory of the readily bioavailable or "fixed" forms of N, primarily nitrate (NO_3^-) and ammonium (NH_4^+), is ultimately governed by the balance between denitrification predominantly in oxygen minimum zones (OMZs) and N fixation by diazotrophs mainly in the (sub)tropical gyres (4–6). Importantly, these processes are connected on a global scale, as an increased loss of fixed N relative to phosphorus (P) favors diazotrophs that perform the energetically costly process of N fixation. As such, the marine N cycle shapes modern nutrient and ecosystem dynamics and in this system of negative feedbacks, the N:P ratio and hence fixed-N inventory of the ocean are tightly regulated. Known as the "nitrostat," these feedbacks are assumed to have been relatively stable since the origin of diazotrophs in the Archaean (7) and subsequent proliferation during the (Late) Proterozoic (5).

This assumption that strong negative feedbacks stabilize the oceanic N inventory, speciation, and productivity tends to frame our interpretation of future scenarios (8) and past events (9), including oceanic anoxic events (OAEs). The OAEs occurred predominantly during the Mesozoic and are associated with widespread ocean deoxygenation and perturbations of major biogeochemical cycles, including the marine N cycle (10). For example, OAEs are

associated with depleted bulk sediment nitrogen isotope ($\delta^{15}N_{bulk}$) values in some parts of the (proto-) Atlantic Ocean (11, 12). The classical hypothesis for the operation of the marine N cycle in an extremely deoxygenated ocean—such as occurred during the OAEs—argues that primary production was dominated by diazotrophs (12, 13) to counter the high rates of N loss in the expanded OMZs, resulting in low $\delta^{15}N_{bulk}$ values. This would be generally consistent with our understanding of a dominance of nitrostat-driven negative feedbacks between denitrification and N fixation in the modern oceans, stabilizing the oceanic inventory of fixed N (1, 2, 4).

However, the very negative ($<-2‰$) $\delta^{15}N_{bulk}$ and even more depleted ($<-4‰$) chlorophyll-derived porphyrin N isotopes ($\delta^{15}N_{por}$) from the (equatorial) Atlantic across OAE 2 suggest a contribution, potentially major, from eukaryotic primary producers assimilating recycled ammonium (11, 14, 15). This hints at a very different operation of the marine N cycle under conditions of extreme ocean deoxygenation, in which ammonium availability may be high enough to play a major role in regulating export production, at least in the equatorial Atlantic. Similarly, very depleted $\delta^{15}N_{bulk}$ (minima ~ $-3‰$) have been found in semirestricted shelf

Significance

The ratio of the dissolved inventories of readily bioavailable (fixed) nitrogen to phosphorus is regulated close to 16:1 in the modern, well-oxygenated ocean. This situation—fixed-nitrogen tracking phosphorus—is generally assumed to have operated for hundreds of millions of years. Here we use computer simulations combined with proxy data to instead demonstrate that the marine nitrogen cycle operates very differently when dissolved oxygen concentrations in the ocean are considerably lower than present. Not only is nitrate replaced by ammonium as the dominant component of fixed nitrogen, but the total fixed inventory collapses relative to phosphorus. This makes the strength and state of the biological pump in the ocean highly susceptible to disruption, with potential past and future implications.

basins of the Tethys Ocean during the Paleocene Eocene Thermal Maximum (PETM) (16), suggesting an important role for ammonium assimilation during this transient global warming event. Together, these observations suggest that ammonium assimilation might be inherent to deoxygenation events during the Phanerozoic and may reflect the changing balance in redox speciation of the major components of dissolved inorganic nitrogen (DIN), namely: NO_3^- and NH_4^+ (together: the fixed-nitrogen pool).

However, these observations highlight a major challenge: resolving the role and strength of marine N-cycle feedbacks is complicated by the fact that evidence recorded in the sediments is fragmented and reflects local, not global processes (17). For OAE 2, virtually all proxy data are from the (central) Atlantic and Tethys Ocean (11). In addition, the proxy record predominantly reflects surface ocean processes, limiting our understanding of N-cycle dynamics in the ocean's interior and hence the dominant reservoir of N in the intermediate and deep ocean; upwelling of this deep reservoir supports much of primary production in modern systems, and presumably in ancient ones as well. Furthermore, although models have been used to study the marine N cycle during OAE 2 (11, 15), these models have tended to either focus on a regional scale, and the area of the (proto-) Atlantic and Tethys Ocean (11), or only on the average surface vs. average deep ocean (15). Assessment of the marine N-cycle dynamics in a fully 3-dimensional and global context, as well as a more generalized understanding of how global N cycling responds
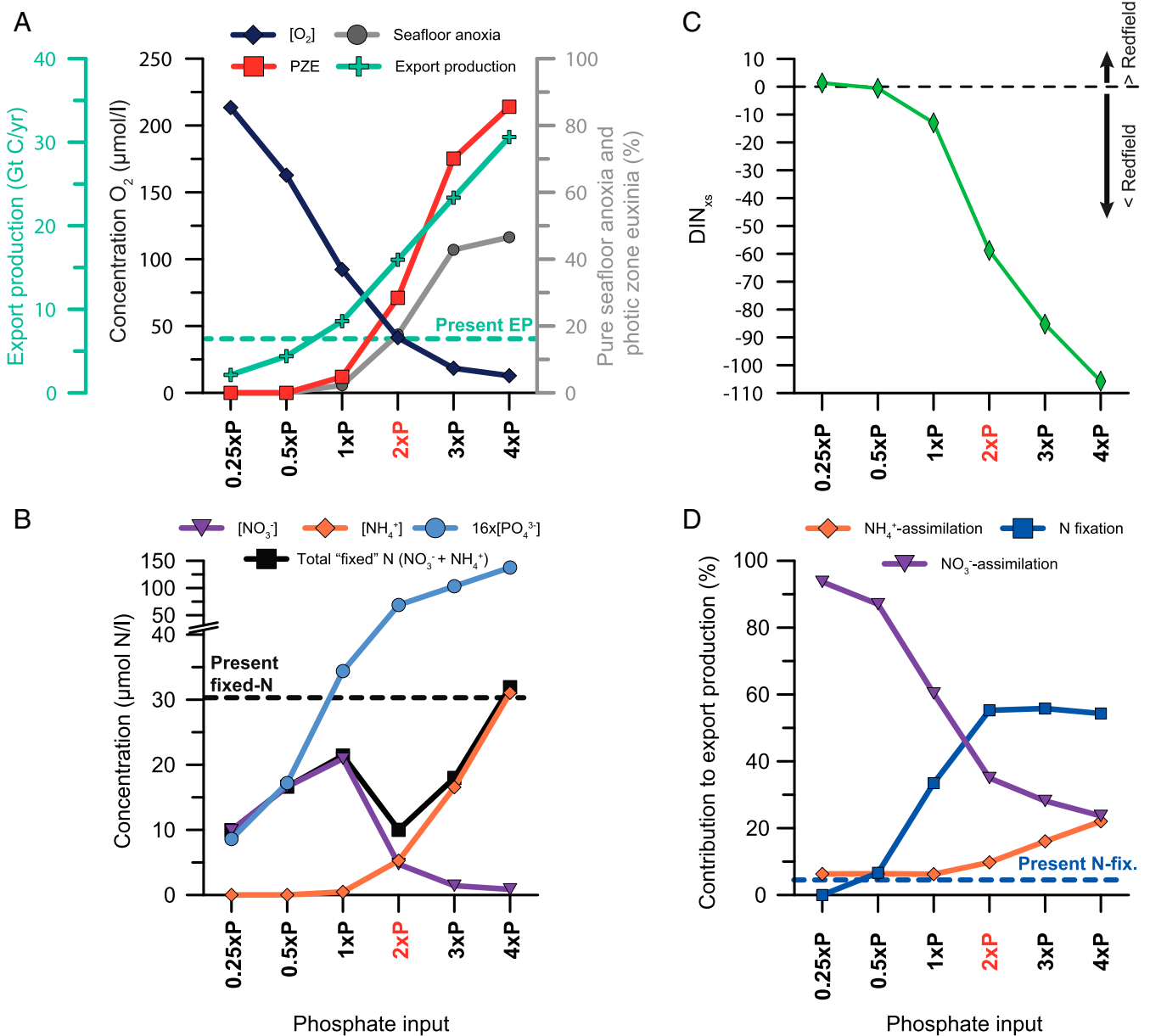

Fig. 1. Response of marine biogeochemistry. Response of ocean biogeochemistry to an increase in oceanic phosphate inventory for the Cenomanian simulations (pCO$_2$ at 1,120 ppmv). (*A*) Ocean redox state with total oxygen content (O$_2$) of the ocean, extent of PZE, extent of pure sea-floor anoxia (<1 nM O$_2$), and rate of export production; (*B*) Concentration of nitrate, ammonium, total fixed nitrogen (NO$_3^-$ + NH$_4^+$), and phosphate concentration (in μmol N l^{-1}; multiplied by the Redfield N:P ratio); (*C*) DIN$_{xs}$ (DIN$_{xs}$ = NO$_3^-$ + NH$_4^+$ − 16 × PO$_4^{3-}$) (38), and (*D*) Contribution of nitrogen fixation, ammonium assimilation, and nitrate assimilation to export production. Dashed lines represent values in modern-day simulation (1 × CO$_2$, 1 × PO$_4^{3-}$, and modern geography, ocean circulation, and temperature). The 2 × PO$_4^{3-}$ simulation has the best fit with proxy data for OAE 2 (25).

Table 1. Marine biogeochemistry for the modern and (pre)OAE 2

Variable	Unit	Modern (Observed)	Modern (GENIE)	Pre-OAE 2 (GENIE)	OAE 2 (GENIE)
Atmospheric CO_2		$1 \times CO_2$	$1 \times CO_2$	$2 \times CO_2$	$4 \times CO_2$
Oceanic phosphate		$1 \times PO_4^{3-}$	$1 \times PO_4^{3-}$	$1 \times PO_4^{3-}$	$2 \times PO_4^{3-}$
Anoxia					
Global ocean anoxia	% volume	<0.1 (ref. 39)	<0.1	2	11
Seafloor anoxia	% area	<0.1 (ref. 39)	<0.1	2	17
Euxinia					
Global ocean euxinia	% volume	<0.1 (ref. 39)	<0.1	4	28
Photic zone euxinia	% area	<0.1 (ref. 39)	<0.1	0.5	11
Biological rates					
Export production	Gt C y^{-1}	5–20 (ref. 40)	7	8	16
Nitrification	Tg N y^{-1}		2,312	3,152	6,050
Denitrification	Tg N y^{-1}	120–240 (ref. 41)	114	812	3,249
Global contribution to export					
NO_3 assimilation	%		87	65	35
N_2 fixation	%		5	28	55
NH_4^+ assimilation	%		8	6	10
Global contribution to remineralization					
O_2 respiration	%		99	90	72
Denitrification	%		1	8	16
SO_4^{2-} reduction	%		<0.1	2	12

to extreme ocean deoxygenation events, is still needed. To elucidate global-scale marine N-cycle dynamics as the ocean is progressively deoxygenated, here we used an Earth System model of intermediate complexity ("GENIE") (18) and as a case study used Cenomanian–Turonian OAE 2 (~93 Ma), one of the most extreme ocean deoxygenation events of the last 250 Ma.

Results

In our simulations, as the oceanic P inventory increases, the associated increase in export production causes the oxygen content of the ocean to decrease, leading to expanded anoxia, here defined as <1 nM O_2 (Fig. 1A). All simulations with more than $1 \times PO_4^{3-}$ have enhanced export production and an expanded extent of photic zone euxinia (PZE) compared to modern, in agreement with previous box-model studies (e.g., refs. 19 and 20). In the highest ($4 \times PO_4^{3-}$) scenario, export production is more than 4× higher than modern rates (Fig. 1A), and the upper-depth boundaries of the OMZs impinge on the photic zone, leading to PZE in ~35% of the ocean. Within the euxinic OMZs, organic matter remineralization is predominantly mediated by sulfate reduction, contributing to 21% of total OM remineralization globally (*SI Appendix*, Fig. S3).

Our P inventory-induced changes in the extent of ocean oxygenation have a profound impact on the marine N cycle, and in particular, on which species of N dominates the fixed nitrogen pool: nitrate or ammonium. In our model, an increase from 0.25 to $1 \times PO_4^{3-}$ concentration enhances primary production ~4-fold, from 2.2 to 8.6 Gt C y^{-1}, and leads to an increase in the fixed N inventory (NO_3^- + NH_4^+) of the ocean by around 200% due to a compensating increase in N fixation (Fig. 1 B–D). Notably, this is far short of the 400% increase that would have been necessary to maintain a mean N:P ocean inventory of 16:1, the reasons for which we discuss later. The marine N cycle in the $1 \times PO_4^{3-}$ simulation ($4 \times CO_2$, and Cenomanian paleogeography) differs from the results for the modern (Table 1). In our Cenomanian simulations, the fixed-N inventory does not reach modern values until the $4 \times PO_4^{3-}$ simulations (Fig. 1B), highlighting the role of atmospheric CO_2 and paleogeography (affecting temperature and ocean currents, respectively) in modulating the state of marine N cycling, in addition to changes in the oceanic P inventory. In the Cenomanian simulation, higher temperatures and different ocean circulation deplete the N inventory compared to

modern (Fig. 1C), implying that future warmer, deoxygenated conditions could also reduce the global ocean N inventory.

As concentrations increase toward $4 \times PO_4^{3-}$, the fraction of the ocean that is anoxic expands, and denitrification rates increase, resulting in up to ~15% of global organic matter being remineralized via NO_3^- respiration. The value of ~15% appears to be an inherent limit for the global contribution of denitrification to organic remineralization (*SI Appendix*, Fig. S3). This, in turn, places a limit on the loss of fixed N and ultimately leads to a maximum contribution of N fixation to export production of ~55–60% for an ocean with widespread anoxia but operating under an oxygen-rich atmosphere (Fig. 1D). This limit is due to geographic restriction of denitrification, which mainly occurs at the edge of the OMZs, where oxygen is low enough for denitrification, yet nitrification rates remain high enough to produce nitrate. As oxygen content in the ocean decreases, higher rates of denitrification, combined with lower nitrification rates, result in a sharp decline in nitrate concentration, reducing the eventual contribution of upwelled nitrate to export production (Fig. 1 B–D).

Because nitrification of NH_4^+ requires oxygen, NH_4^+ accumulates in the ocean, mostly in the OMZs. In the $4 \times PO_4^{3-}$ ocean, average NH_4^+ concentrations reach up to 2 orders of magnitude higher than in the modern ocean (Fig. 1B), reaching values similar to those observed in the modern OMZ of the Black Sea (21). In such an "ammonium ocean," NH_4^+ assimilation does not dominate the source of nutrient nitrogen for export production globally, constituting at most 22% of total export production (Fig. 1D). This is because most of the upwelled NH_4^+ is nitrified in oxygenated layers underlying the photic zone. However, where local NH_4^+ assimilation occurs, it can contribute >30% of export production, for example in the tropical proto-Atlantic. The relative contribution of N fixation and NH_4^+ assimilation to export production is thus controlled by the spatial structure of the OMZ relative to the base of the photic zone, which in turn is controlled by ocean circulation (i.e., upwelling regions). When the OMZ impinges the photic zone, NH_4^+ becomes available for direct assimilation by phytoplankton. When the OMZ is spatially separated from the photic zone, nitrification (and subsequent denitrification) reduce the availability of NH_4^+ to the photic zone.

However, our results collectively demonstrate that the system does not monotonically transition from a "nitrate-" to an ammonium ocean as oxygen progressively declines. Under intermediate
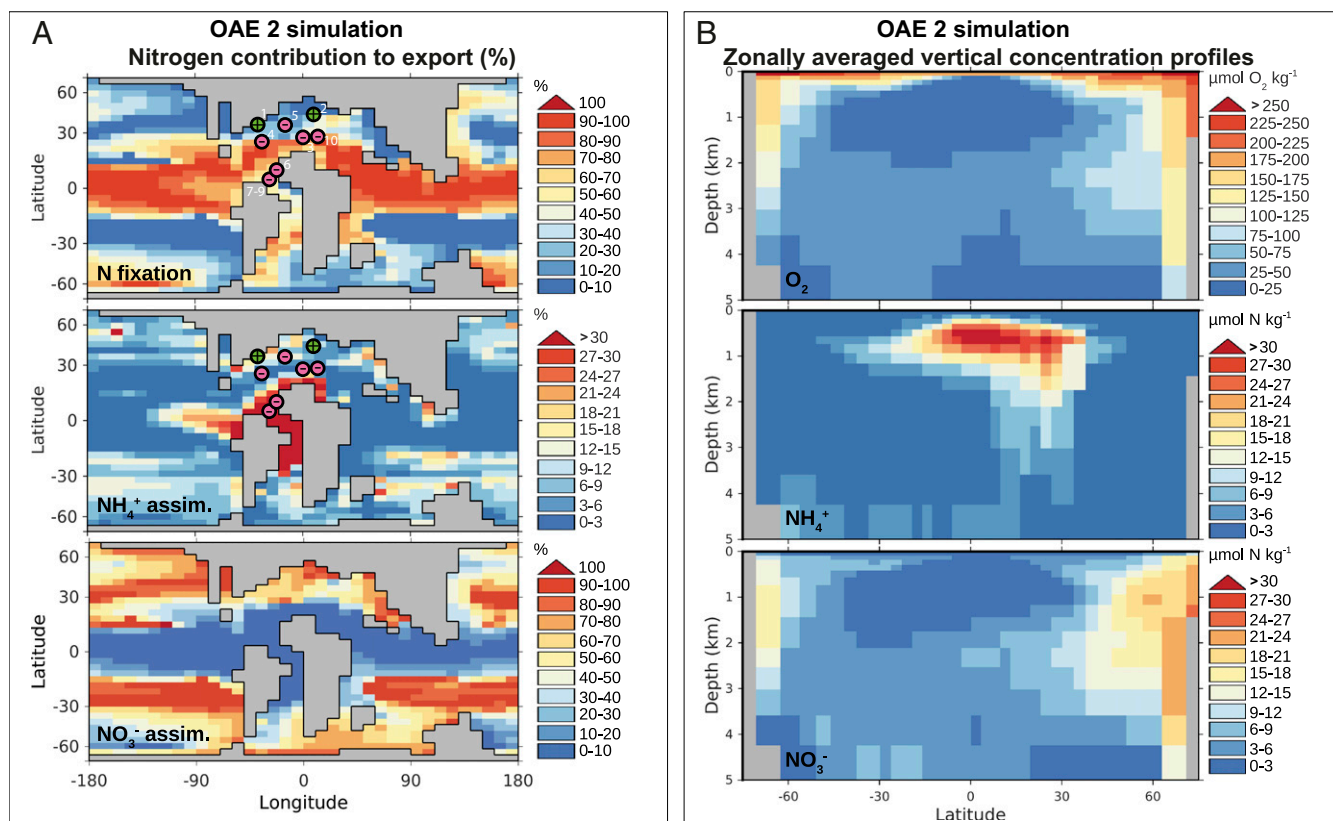
Fig. 2. Marine N cycle during OAE 2 ($4 \times CO_2$; $2 \times PO_4^{3-}$). (*A*) Spatial distribution of the relative contribution to export production of N fixation (*Top*), NH_4^+ assimilation (*Middle*), and NO_3^- assimilation (*Bottom*). Green ⊕ symbols reflect proxy records with a positive average $\delta^{15}N_{bulk}$ value across OAE 2, while pink ⊖ symbols reflect a negative average $\delta^{15}N_{bulk}$ value. Numbers refer to sites listed in *SI Appendix*, Table S1 (see *SI Appendix* for details); and (*B*) zonally averaged vertical concentration profiles of O_2 (*Top*), NH_4^+ (*Middle*), and NO_3^- (*Bottom*). Both panels present model results using the OAE 2 analog simulation (Cenomanian paleography, $4 \times CO_2$; $2 \times PO_4^{3-}$).

conditions in the transition (in our Cenomanian simulations: $2 \times PO_4^{3-}$), a unique state of N cycling occurs in which the ocean is not yet anoxic enough to develop extensive OMZs rich in ammonium. Relatively high rates of nitrification restrict the accumulation of NH_4^+, yet at the same time, high rates of denitrification keep the ocean nitrate inventory low (Fig. 1*D*). As a result, the ocean becomes extremely depleted in all forms of fixed N (Fig. 1*B*).

Discussion

Contrary to earlier studies (22, 23), our results show how the deep ocean can become highly depleted in fixed N relative to P, leading to a biogeochemical state that contrasts markedly to the modern oxic ocean. As P concentrations increase and anoxia expands, the ocean transitions from a feedback-balanced system where the nitrate inventory tracks phosphate (24), to a state in which the deep ocean becomes highly depleted in fixed N relative to P (Fig. 1*C*). And, rather than a NO_3^--replete deep ocean (Fig. 3*A*), the dominant form of nitrogen becomes NH_4^+, which is furthermore localized to expanded OMZs and does not "fill" all of the deep ocean (Table 1 and Fig. 3 *B* and *C*). This transformation occurs in the model despite high rates of N fixation at the surface by diazotrophs and concomitantly high export production fluxes of particulate organic nitrogen into the ocean interior—both factors that should favor a large deep-ocean fixed-N inventory of NH_4^+ released from organic matter remineralization.

But, did an ocean state such as this really develop in the past? Proxy data for bottom water anoxia and photic zone euxinia during OAE 2 best match the $2 \times PO_4^{3-}$ simulation (25). Although there are a number of uncertainties and caveats associated with both the model simulations and proxy data, the $2 \times PO_4^{3-}$ scenario also is

the same scenario that yields a marine N-cycle simulation with minimum total fixed-N inventory (Fig. 1*B*). In this simulation, 11% of the total volume of the ocean and 17% of the seafloor is anoxic (defined here as <1 nM O_2) (Fig. 1*A* and Table 1), consistent with uranium isotope data that indicate that 8–15% of the seafloor became anoxic during OAE 2 (26). We argue that the existence of an elevated oceanic P inventory compared to the modern is consistent with calcium isotope measurements. The calcium isotope data indicate an increased weathering flux during OAEs (27) and as total calcium and P concentrations can be correlated in modern rivers (28), presumably reflect an increased rate of PO_4^{3-} supply to the ocean. Together with the likelihood that P was more strongly regenerated from the ocean floor under anoxic conditions (29), an increased PO_4^{3-} state is a reasonable outcome, and the relatively conservative $2 \times PO_4^{3-}$ amplification (rather than $3 \times$ or $4 \times PO_4^{3-}$) is the scenario that leads to the greatest reduction in fixed-N inventory.

In the $2 \times PO_4^{3-}$ simulations, N fixation is the most intense in equatorial upwelling regions and in the Pacific sector of the Southern Ocean, where deep and denitrified waters with low N:P ratios reach the photic zone (Fig. 2). Globally, NH_4^+ assimilation is significant but is not the dominant source of nutrient nitrogen for marine production, contributing ~10% of total export production (Table 1). Regionally, however, NH_4^+-assimilation is important in the most intensely anoxic and/or upwelling regions, such as the euxinic equatorial Atlantic (Fig. 2).

Available nitrogen stable isotope data for OAE 2 allow for comparison with our model simulations, although published data to date are restricted to the (proto)-Atlantic and Tethys Ocean. Records from the equatorial Atlantic (Demerara Rise sites and
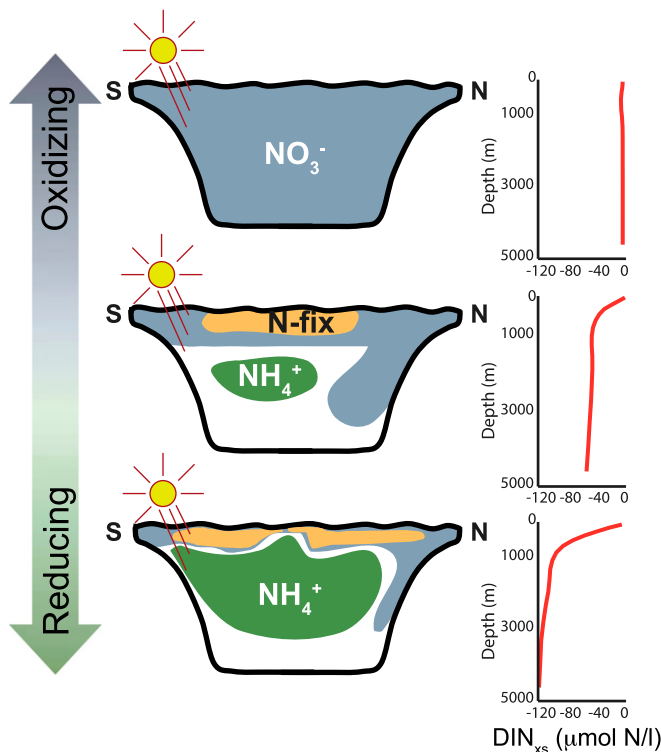
Fig. 3. Schematic of the marine nitrogen cycle's response to oceanic deoxygenation. The transition from an oxic, nitrate-dominated ocean to an anoxic, ammonium-dominated ocean. Also shown is DIN_{xs} ($DIN_{xs} = NO_3^- + NH_4^+ - 16 \times PO_4^{3-}$) (38). During OAE 2, the intermediate N-deficit state may have prevailed.

Site 367) show extremely depleted $\delta^{15}N_{bulk}$ values during OAE 2, with minima of $<-3‰$ and average values around $-2‰$ (13–15). These depleted $\delta^{15}N$ values are interpreted to reflect a region dominated by N fixation and/or NH_4^+ assimilation, although it is difficult to disentangle the individual importance of these two processes (15). Our model simulations are in concordance, with a relatively large contribution of N fixation and especially NH_4^+ assimilation (>30%), to export production in this region (Fig. 2*A*). By contrast, the continental margins of Europe and North America are characterized by enriched ($\delta^{15}N_{bulk}$ values around $1‰$), even during the peak of OAE 2 (11). This is also consistent with our simulations, which indicate a low contribution of N fixation and NH_4^+ assimilation to export production on those particular margins, with productivity instead dominated by NO_3^-. Sites in the subtropical Atlantic (Sites 386, 1276, and 641) (11) are characterized by negative $\delta^{15}N_{bulk}$ values (average values around $-1‰$), although less negative than those recorded in the equatorial Atlantic (averages around $-2‰$). Our simulations are largely consistent with these intermediate $\delta^{15}N_{bulk}$ values, as the surface ocean at Sites 368 and 641 is characterized by a high contribution of N fixation to export production (>50%), but no major influence of ammonium assimilation. Site 1276 is an exception to the general agreement between our model simulations and published interpretations of $\delta^{15}N_{bulk}$ proxy data. In our simulations, this location is not characterized by high contributions of N fixation and/or NH_4^+ assimilation that would lead to depleted $\delta^{15}N_{bulk}$, yet the available $\delta^{15}N_{bulk}$ values are negative. This could be because the resolution of cGENIE is insufficient to reconstruct small-scale features in ocean circulation or biology that drive the $\delta^{15}N_{bulk}$ values at Site 1276 negative. But, overall our simulations compare well with the proxy record from the Atlantic and Tethys Ocean as well as regional box-modeling studies (11, 14, 15, 30), providing additional confidence.

Both the proxy record and previous box-modeling studies are limited to the Atlantic and Tethys Ocean. Our global ocean simulations suggest that NH_4^+ assimilation may have fueled export production in parts of the eastern equatorial Pacific, and that N fixation was important across the equatorial Pacific and Indian Ocean and in the high-latitude southern Pacific Ocean, regions characterized by stronger exchanges between the deep and the surface ocean. However, formal assessment of these model predictions will have to await new data from these basins, and higher-resolution ocean biogeochemical modeling.

If the marine N cycle of OAE 2 can maintain a fundamentally different structure from the modern version, one might expect comparably different N cycle states to occur at other times in Earth history. For example, Late Devonian black shales (31) as well as PETM black shales (16) are characterized by depleted $\delta^{15}N_{bulk}$ values similar to those reported for OAE 2. The climate state and paleogeography, which determine the specific sensitivity of the marine N cycle to changes in oxygenation state, were different during those events compared to OAE 2. However, the same mechanisms and feedback processes identified for the OAE 2 scenario presumably would operate. If the anoxia was intense enough, these events also may have promoted a depletion in bioavailable N; and incorporation of ammonium may have been important in euxinic (semi)-restricted basins (e.g., the northeast Tethys during the PETM).

Changing the global N inventories and spatial patterns of N cycling also has far-reaching implications for marine ecology and attendant proxies, and other biogeochemical cycles. For example, the habitat for ammonia oxidizers (e.g., Thaumarchaeota) may have been very different in a reorganized, low-oxygen N cycle. These organisms may have moved to shallower depths if they were able to resist photoinhibition and other associated oxidative pressures. This shift in habitat may then influence TEX_{86}-based temperature estimates in anoxic basins, as existing calibrations are based on modern systems in which the organisms primarily reside below the base of the photic zone. Marine N_2O production likely would also have increased during anoxic events due to elevated rates of both denitrification and nitrification, and a potential shift between denitrification and anammox (32), which characterize some of the main pathways of N_2O production in the ocean (33). If the N_2O cycle shifted closer to surface waters, thereby increasing gas evasion rates, N_2O could have provided a powerful positive feedback mechanism to sustain the OAE. N_2O is a potent greenhouse gas, 1,000× more effective than CO_2, and its release could partially offset the negative feedback on warming of the expansion in organic carbon burial. The interplay of such processes could account for the rather complex temperature changes observed across OAE 2 (34). Besides the biogeochemical implications, these changes in the marine N cycle likely also impacted marine trophic structures and food webs and could be an important mechanism for how deoxygenation events such as the OAEs drive biological turnover

The scenarios modeled here may also have important implications for future climate change. Over the past 50 y the oxygen content of the ocean has declined (35) and is expected to accelerate with future ocean warming (36). Some regions of the ocean are already close to transitioning to full anoxia (<10 nM O_2) (37). Our results illuminate the sensitivity of the marine N cycle to changes in ocean oxygen content, implying that the future ocean may be more vulnerable to N loss than previously recognized, which will have far-reaching consequences for other biogeochemical processes and marine ecosystems.

Conclusions

Our understanding of the response of the marine N cycle to changes in ocean oxygenation largely comes from past perturbation events such as the OAEs of the Mesozoic, with relatively sparse proxy records and regional models informing most of our

understanding to date. Here, we applied an Earth system model with 3D global ocean (GENIE), upgraded with a more complete set of N-cycle processes, to provide specific insights into the global marine N cycle associated with OAE 2 as well as to provide generalized understanding of how the marine N cycle responds under progressively extreme deoxygenation. We find that as phosphate concentrations increase and anoxia expands, the ocean transitions from an oxic state with high concentrations of nitrate to an anoxic/reducing state in which the deep ocean becomes highly depleted in fixed N relative to P, with N predominantly in the form of ammonium and mostly geographically restricted to expanded OMZs. These results point to potential breakdown in the feedbacks that were thought to keep global N marine inventories in balance, i.e., the nitrostat.

Materials and Methods

All simulations were run using the GENIE model. As employed here, GENIE includes representations of the marine cycles of phosphorus, nitrogen, oxygen, and sulfur. To extend the applicability of GENIE to a poorly oxygenated ocean, we further developed the N cycle to include second-order substrate limitation of nitrification rates by both ammonium and oxygen rather than just ammonium (*SI Appendix*).

1. M. Voss *et al.*, The marine nitrogen cycle: Recent discoveries, uncertainties and the potential relevance of climate change. *Philos. Trans. R. Soc. Lond. B Biol. Sci.* **368**, 20130121 (2013).
2. C. M. Moore *et al.*, Processes and patterns of oceanic nutrient limitation. *Nat. Geosci.* **6**, 701–710 (2013).
3. P. G. Falkowski, R. T. Barber, V. Smetacek, Biogeochemical controls and feedbacks on ocean primary production. *Science* **281**, 200–207 (1998).
4. A. C. Redfield, The biological control of chemical factors in the environment. *Am. Sci.* **46**, 205–221 (1958).
5. T. Tyrrell, The relative influences of nitrogen and phosphorus on oceanic primary production. *Nature* **400**, 525–531 (1999).
6. C. Deutsch, J. L. Sarmiento, D. M. Sigman, N. Gruber, J. P. Dunne, Spatial coupling of nitrogen inputs and losses in the ocean. *Nature* **445**, 163–167 (2007).
7. E. E. Stüeken, R. Buick, B. M. Guy, M. C. Koehler, Isotopic evidence for biological nitrogen fixation by molybdenum-nitrogenase from 3.2 Gyr. *Nature* **520**, 666–669 (2015).
8. N. Gruber, J. N. Galloway, An Earth-system perspective of the global nitrogen cycle. *Nature* **451**, 293–296 (2008).
9. R. A. Boyle *et al.*, Nitrogen cycle feedbacks as a control on euxinia in the mid-Proterozoic ocean. *Nat. Commun.* **4**, 1533 (2013).
10. H. C. Jenkyns, Geochemistry of oceanic anoxic events. *Geochem. Geophy. Geosy.* **11**, Q03004 (2010).
11. I. Ruvalcaba Baroni, N. A. G. M. van Helmond, I. Tsandev, J. J. Middelburg, C. P. Slomp, The nitrogen isotope composition of sediments from the proto-North Atlantic during Oceanic Anoxic Event 2. *Paleoceanography* **30**, 923–937 (2015).
12. G. H. Rau, M. A. Arthur, W. E. Dean, $^{15}N/^{14}N$ variations in cretaceous Atlantic sedimentary sequences: Implication for past changes in marine nitrogen biogeochemistry. *Earth Planet. Sci. Lett.* **82**, 269–279 (1987).
13. M. M. M. Kuypers, Y. van Breugel, S. Schouten, E. Erba, J. S. Sinninghe Damsté, N_2-fixing cyanobacteria supplied nutrient N for Cretaceous oceanic anoxic events. *Geology* **32**, 853–856 (2004).
14. C. K. Junium, M. A. Arthur, Nitrogen cycling during the cretaceous, Cenomanian-Turonian Oceanic Anoxic Event II. *Geochem. Geophy. Geosy.* **8**, Q03002 (2007).
15. M. B. Higgins, R. S. Robinson, J. M. Husson, S. J. Carter, A. Pearson, Dominant eukaryotic export production during ocean anoxic events reflects the importance of recycled NH_4^+. *Proc. Natl. Acad. Sci. U.S.A.* **109**, 2269–2274 (2012).
16. C. K. Junium, A. J. Dickson, B. T. Uveges, Perturbation to the nitrogen cycle during rapid Early Eocene global warming. *Nat. Commun.* **9**, 3186 (2018).
17. J. Trabucho-Alexandre *et al.*, The mid-Cretaceous North Atlantic nutrient trap: Black shales and OAEs. *Paleoceanography* **25**, PA4201 (2010).
18. A. Ridgwell *et al.*, Marine geochemical data assimilation in an efficient Earth System Model of global biogeochemical cycling. *Biogeosciences* **4**, 87–104 (2007).
19. I. Tsandev, C. P. Slomp, Modeling phosphorus cycling and carbon burial during Cretaceous Oceanic Anoxic Events. *Earth Planet. Sci. Lett.* **286**, 71–79 (2009).
20. S. Flögel *et al.*, Simulating the biogeochemical effects of volcanic CO_2 degassing on the oxygen-state of the deep ocean during the Cenomanian/Turonian Anoxic Event (OAE 2). *Earth Planet. Sci. Lett.* **305**, 371–384 (2011).
21. S. K. Konovalov, L. I. Ivanov, A. S. Samodurov, Oxygen, nitrogen and sulphide fluxes in the Black Sea. *Mediterr. Mar. Sci.* **1**, 41–59 (2000).
22. K. Fennel, M. Follows, P. G. Falkowski, The co-evolution of the nitrogen, carbon and oxygen cycles in the Proterozoic ocean. *Am. J. Sci.* **305**, 526–545 (2005).
23. M. R. Saltzman, Phosphorus, nitrogen, and the redox evolution of the Paleozoic oceans. *Geology* **33**, 573–576 (2005).
24. T. M. Lenton, A. J. Watson, Redfield revisited: 1. Regulation of nitrate, phosphate, and oxygen in the Ocean. *Global Biogeochem. Cycles* **14**, 225–248 (2000).
25. F. M. Monteiro, R. D. Pancost, A. Ridgwell, Y. Donnadieu, Nutrients as the dominant control on the spread of anoxia and euxinia across the Cenomanian-Turonian oceanic anoxic event (OAE2): Model-data comparison. *Paleoceanography* **27**, PA4209 (2012).
26. M. O. Clarkson *et al.*, Uranium isotope evidence for two episodes of deoxygenation during Oceanic Anoxic Event 2. *Proc. Natl. Acad. Sci. U.S.A.* **115**, 2918–2923 (2018).
27. C. L. Blättler, H. C. Jenkyns, L. M. Reynard, G. M. Henderson, Significant increases in global weathering during Oceanic Anoxic Events 1a and 2 indicated by calcium isotopes. *Earth Planet. Sci. Lett.* **309**, 77–88 (2011).
28. W. A. House, F. H. Denison, Total phosphorus content of river sediments in relationship to calcium, iron and organic matter concentrations. *Sci. Total Environ.* **282-283**, 341–351 (2002).
29. P. Van Cappellen, E. D. Ingall, Benthic phosphorus regeneration, net primary production, and ocean anoxia: A model of the coupled marine biogeochemical cycles of carbon and phosphorus. *Paleoceanography* **9**, 677–692 (1994).
30. I. Ruvalcaba Baroni, I. Tsandev, C. P. Slomp, Enhanced N_2-fixation and NH^{4+} recycling during oceanic anoxic event 2 in the proto-North Atlantic. *Geochem. Geophys. Geosyst.* **15**, 4064–4078 (2014).
31. M. L. Tuite, Jr, S. A. Macko, Basinward nitrogen limitation demonstrates role of terrestrial nitrogen and redox control of δ15N in a Late Devonian black shale. *Geology* **41**, 1079–1082 (2013).
32. R. Buick, Did the Proterozoic 'Canfield Ocean' cause a laughing gas greenhouse? *Geobiology* **5**, 97–100 (2007).
33. A. Freing, D. W. R. Wallace, H. W. Bange, Global oceanic production of nitrous oxide. *Philos. Trans. R. Soc. Lond. B Biol. Sci.* **367**, 1245–1255 (2012).
34. U. Heimhofer *et al.*, Vegetation response to exceptional global warmth during Oceanic Anoxic Event 2. *Nat. Commun.* **9**, 3832 (2018).
35. S. Schmidtko, L. Stramma, M. Visbeck, Decline in global oceanic oxygen content during the past five decades. *Nature* **542**, 335–339 (2017).
36. L. Bopp *et al.*, Multiple stressors of ocean ecosystems in the 21st century: Projections with CMIP5 models. *Biogeosciences* **10**, 6225–6245 (2013).
37. L. A. Bristow *et al.*, N_2 production rates limited by nitrite availability in the Bay of Bengal oxygen minimum zone. *Nat. Geosci.* **10**, 24–29 (2016).
38. D. A. Hansell, N. R. Bates, D. B. Olson, Excess nitrate and nitrogen fixation in the North Atlantic Ocean. *Mar. Chem.* **84**, 243–265 (2004).
39. H. E. Garcia *et al.*, *World Ocean Atlas 2013, Volume 3: Dissolved Oxygen, Apparent Oxygen Utilization, and Oxygen Saturation*, S. Levitus, A. Mishonov, Eds. (NOAA Atlas NESDIS, National Oceanic and Atmospheric Administration, Silver Spring, MD, 2014).
40. S. A. Henson *et al.*, A reduced estimate of the strength of the ocean's biological carbon pump. *Geophys. Res. Lett.* **38**, L04606 (2011).
41. T. DeVries, C. Deutsch, P. A. Rafter, F. Primeau, Marine denitrification rates determined from a global 3-D inverse model. *Biogeosciences* **10**, 2481–2496 (2013).